JCTC Journal of Chemical Theory and Computation

Letter

pubs.acs.org/JCTC

Resolutions of the Coulomb Operator:† VII. Evaluation of Long-Range Coulomb and Exchange Matrices

Taweetham Limpanuparb,*[,‡,§] Josh Milthorpe,[‡] Alistair P. Rendell,[‡] and Peter M. W. Gill[∥]

[‡]Research School of Computer Science, Australian National University, ACT 0200, Australia

[§]Mahidol University International College, Mahidol University, Nakhonpathom 73170, Thailand

[∥]Research School of Chemistry, Australian National University, ACT 0200, Australia

ABSTRACT: Use of the resolution of Ewald operator method for computing long-range Coulomb and exchange interactions is presented. We show that the accuracy of this method can be controlled by a single parameter in a manner similar to that used by conventional algorithms that compute two-electron integrals. Significant performance advantages over conventional algorithms are observed, particularly for high quality basis sets and globular systems. The approach is directly applicable to hybrid density functional theory.

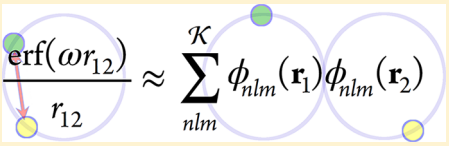

1. INTRODUCTION

The partitioning of the Coulomb operator $(1/r_{12})$ into a short-range part and a smooth long-range part is central to long-range corrected density functional theory (LRC-DFT) methods[7−15] such as CAM-B3LYP,[8] HSE,[9−12] LCgau-BOP,[13] LC-ωPBE,[14] and ωB97XD.[15] It also naturally allows for different computational techniques to be applied to the two different components, and this in turn can lead to performance gains. Noting that with such a partitioning the short-range component can be evaluated at a relatively small computational cost,[10,16−20] the focus of this Letter is on computing the long-range part. Specifically, we consider computing Hartree−Fock Coulomb and exchange interactions for the long-range Ewald operator

$$L(r_{12}) = \frac{\mathrm{erf}(\omega r_{12})}{r_{12}} \tag{1}$$

with values for ω (0.1−0.5) that reflect those commonly used in LRC-DFT implementations.[8−15]

In previous work it was shown that a two-electron operator like eq 1 may be resolved[1−6,21,22] into a sum of products of one-electron functions

$$L(r_{12}) = \sum_{n=0}^{\infty}\sum_{l=0}^{\infty}\sum_{m=-l}^{l} \phi_{nlm}(\mathbf{r}_1)\phi_{nlm}(\mathbf{r}_2) \equiv \sum_{k=1}^{\infty} \phi_k(\mathbf{r}_1)\phi_k(\mathbf{r}_2) \tag{2}$$

In practice, we truncate the resolution (eq 2) to a $\mathcal{K}$-term finite sum

$$L(r_{12}) \approx \sum_{n=0}^{\mathcal{N}'}\sum_{l=0}^{\mathcal{L}}\sum_{m=-l}^{l} \phi_{nlm}(\mathbf{r}_1)\phi_{nlm}(\mathbf{r}_2) \equiv \sum_{k=1}^{\mathcal{K}} \phi_k(\mathbf{r}_1)\phi_k(\mathbf{r}_2) \tag{3}$$

where

$$k = n(\mathcal{L}+1)^2 + l(l+1) + m + 1$$

and

$$\mathcal{K} = (\mathcal{N}'+1)(\mathcal{L}+1)^2$$

As a result, the long-range two-electron integrals (assuming real basis functions)

$$(\mu\nu|\lambda\sigma) = \iint \chi_\mu(\mathbf{r}_1)\chi_\nu(\mathbf{r}_1)L(\mathbf{r}_{12})\chi_\lambda(\mathbf{r}_2)\chi_\sigma(\mathbf{r}_2)\,\mathrm{d}\mathbf{r}_1\,\mathrm{d}\mathbf{r}_2 \tag{4}$$

can be represented by a sum of products of one-electron overlap integrals

$$(\mu\nu|\lambda\sigma) \approx \sum_{nlm}^{\mathcal{K}} (\mu\nu|nlm)(nlm|\lambda\sigma) \tag{5}$$

That is, the traditional calculation of long-range two-electron integrals can be replaced by the calculation of the auxiliary integrals

$$(\mu\nu|nlm) = \int \chi_\mu(\mathbf{r})\chi_\nu(\mathbf{r})\phi_{nlm}(\mathbf{r})\,\mathrm{d}\mathbf{r} \tag{6}$$

In this Letter, we outline the recursion relations used to compute the auxiliary integrals (eq 6), show how the accuracy of this method can be controlled using a single threshold parameter, and provide preliminary performance data that compare this new approach with the traditional approach of evaluating two-electron integrals. This evaluation is performed in the context of computing long-range Coulomb and exchange energies for Hartree−Fock wave functions.

The closed-shell Hartree−Fock Coulomb and exchange matrices are given by

$$J_{\mu\nu} = 2\sum_{a}^{\mathrm{occ}}\sum_{\lambda\sigma}^{N^2} c_{\lambda a}c_{\sigma a}(\mu\nu|\lambda\sigma) \tag{7}$$

Received: December 19, 2012

†Previous papers in the series can be found in refs 1−6

 © XXXX American Chemical Society dx.doi.org/10.1021/ct301110y | J. Chem. Theory Comput. XXXX, XXX, XXX−XXX

$$K_{\mu\nu} = 2\sum_{a}^{\text{occ}}\sum_{\lambda\sigma}^{N^2} c_{\lambda a}c_{\sigma a}(\mu\lambda|\sigma\nu) \tag{8}$$

where N is the number of basis functions, $c_{\mu a}$ are the molecular orbital (MO) coefficients, and occ represents the set of O occupied orbitals. Substituting eq 5 into these expressions yields the Resolution of the Coulomb Operator (RO) expressions:

$$J_{\mu\nu} \approx \sum_{nlm}^{\mathcal{K}} (\mu\nu|nlm)D^{nlm} \tag{9}$$

$$D^{nlm} = \sum_{\lambda\sigma}^{N^2} D_{\lambda\sigma}(nlm|\lambda\sigma) \tag{10}$$

$$K_{\mu\nu} \approx 2\sum_{a}^{\text{occ}}\sum_{nlm}^{\mathcal{K}} (\mu a|nlm)(nlm|a\nu) \tag{11}$$

$$(\mu a|nlm) = \sum_{\lambda}^{N} c_{\lambda a}(\mu\lambda|nlm) \tag{12}$$

where $D_{\lambda\sigma}$ is the density matrix. The efficient evaluation of these equations, their accuracy compared to traditional methods, and the speed of the RO method are now considered. We note that eqs 2−12 are also true for full Coulomb and short-range Coulomb operators. Unless otherwise stated, atomic units are used throughout.

2. COMPUTATIONAL CONSIDERATIONS

The resolution function, ϕ_{nlm} in eq 2 can take a myriad of forms. In this Letter, we discuss functions of the form

$$\phi_{nlm}(\mathbf{r}) = q_n j_l(\lambda_n r)Y_{lm}(\mathbf{r}) \tag{13}$$

where j_l is a spherical Bessel function and Y_{lm} is a real spherical harmonic. For long-range Ewald resolution, we precompute $\lambda_n = 2\beta_n\omega$ and $q_n = 4(b_n\omega)^{1/2}$ where β_n and b_n are the positive Hermite roots and weights of $2(\mathcal{N}+1)$-point Gauss−Hermite quadrature.[5,21]

In the following subsections, we describe three computational aspects of the RO **J** and **K** algorithm that arise from the choice of resolution function eq 13. First, the general outline of the algorithm is discussed. Then, an accuracy control mechanism via a single THRESH value is explained. Last, we elaborate on the calculation of auxiliaries, the lowest layer of the algorithm.

2.1. Outline of the Algorithm. We have written a C++ routine to evaluate the auxiliaries (eq 6) and implemented the rest of the HF **J** and **K** matrix calculation in the X10 language, a modern partitioned global address space language which represents data locality in the form of places and supports a task-parallel model of asynchronous activities.[23] We expect that these features will facilitate a future distributed parallel implementation. The algorithm faithfully follows eqs 9−12. To reduce the memory footprint, we place the loop over n in resolution (eq 2) as the outermost loop. For **J** matrix calculation described by eqs 9 and 10, a single loop over a list of significant shell pairs is used instead of double loops over a number of basis functions. For **K** matrix calculation, we employ DGEMM matrix−matrix multiplication from the BLAS library[24] for both eq 11 and 12. A simple pseudocode is shown in the scheme below. (Einstein summation convention is used.) Our full source code[25] is freely available in *Pumja Rasaayani* (Sanskrit for "quantum chemistry"), a program in the ANU-Chem package.[26] All accuracy and timing results given below use X10 version 2.3 and the corresponding tagged version of ANU-Chem.

```
1 For n = 0...N'
2       A_{μ,νlm} ← (μν|nlm)          eq 6
3       // Coulomb matrix
4       D^{lm} ← D_{μν} × A_{μν,lm}   eq 10
5       J_{μν} + = D_{lm} × A_{μν,lm} eq 9
6       // Exchange matrix
7       B_{νlm,a} ← A_{μ,νlm} × c_{μ,a}   eq 12
8       K_{μν} + = B_{μ,lma} × B_{ν,lma}  eq 11
9 next n
```

From the pseudocode, one can infer that the bottleneck is the matrix−matrix multiplications to produce the exchange matrix at lines 7 and 8 costing $O(ON^2\mathcal{K})$ operations. However, these are handled by DGEMM which can be evaluated very efficiently. The memory costs for matrices **A** and **B** are $O(N^2(\mathcal{L}+1)^2)$ and $O(ON(\mathcal{L}+1)^2)$, respectively.

2.2. Accuracy Control. We introduce a single parameter, THRESH, to control the accuracy of the calculation. Given a THRESH value and molecular geometry, we truncate the sum (eq 2) to $\mathcal{N}'$ and $\mathcal{L}$ using the following procedure. First, we determine the radius of a given molecule using,

$$R = \max\{|\mathbf{r}_i| + r_w(i)\} \tag{14}$$

where $\mathbf{r}_i$ is the position of the ith nucleus and $r_w(i)$ is the van der Waals radius of the ith atom. The molecule is translated to minimize the radius R. We then find $\mathcal{N}$ and $\mathcal{N}'$ using formulas modified from Limpanuparb.[6,21]

$$\mathcal{N} = \lceil (\omega R)^2 + 2\omega R(\sqrt{-\log_{10} x} - 1) + 2\rceil \tag{15}$$

$$\mathcal{N}' = \min\left(\left\lceil \frac{2}{\pi}\sqrt{-(\mathcal{N}+1)\ln x} - 1\right\rceil, \mathcal{N}\right) \tag{16}$$

$$x = \frac{\pi}{4\omega}10^{-\text{THRESH}} \tag{17}$$

We finally determine the largest $\mathcal{L}$ that satisfies the following condition.

$$\frac{(q_n j_{\mathcal{L}}(\lambda_n R))^2}{4\pi} \geq \frac{10^{-\text{THRESH}}}{\mathcal{N}'} \tag{18}$$

These $\mathcal{N}'$ and $\mathcal{L}$ are generally sufficient to guarantee a truncation error in the order of $10^{-\text{THRESH}}$ for the approximation eq 3. It should be noted that eqs 15−17 differ slightly from the original paper[5] because we choose to start the summation (eq 3) from $n = 0$ instead of $n = 1$.[21] The default limits for $\mathcal{N}$ and $\mathcal{L}$ in our program are 300 and 200, respectively, but users can lower this manually via an option in a job input file.

2.3. Auxiliaries. This subsection closely mirrors the previous paper[6] in the series but presents a complete set of equations in real form (as opposed to complex form). The auxiliaries (eq 6) are built up from fundamental integrals (eq 19a) by vertical and horizontal recurrence relations. In trivial cases, the fundamental integrals 19a become 19b and 19c when $P = 0$ and $\lambda_n = 0$, respectively.

dx.doi.org/10.1021/ct301110y | J. Chem. Theory Comput. XXXX, XXX, XXX−XXX

$$[\mathbf{00}|nlm]^{(p)} = \left(-\frac{\lambda_n}{2\zeta P}\right)^p G_n^{AB} j_{l+p}(\lambda_n P) Y_{lm}(\mathbf{P}) \tag{19a}$$

$$[\mathbf{00}|nlm]^{(p)} = \delta_{l,0}\left(-\frac{\lambda_n^2}{2\zeta}\right)^p G_n^{AB} \frac{Y_{00}}{(2p+1)!!} \tag{19b}$$

$$[\mathbf{00}|nlm]^{(p)} = \delta_{l,0}\delta_{p,0} G_n^{AB} Y_{00} \tag{19c}$$

Additional quantities required for the fundamental integrals are presented below.

$$Y_{00} = \frac{1}{2\sqrt{\pi}} \tag{20a}$$

$$\zeta = \alpha + \beta \tag{20b}$$

$$\mathbf{P} = \frac{\alpha\mathbf{A} + \beta\mathbf{B}}{\zeta} \tag{20c}$$

$$G_n^{AB} = q_n\left(\frac{\pi}{\zeta}\right)^{3/2} \exp\left[-\frac{\lambda_n^2}{4\zeta} - \frac{\alpha\beta}{\zeta}|\mathbf{A}-\mathbf{B}|^2\right] \tag{20d}$$

We use the following derivative properties of real solid harmonics $R_{lm}(\mathbf{r}) = r^l Y_{lm}(\mathbf{r})$

$$\partial_x R_{lm} = c_{lm}^{x+} R_{l-1,m+1} + c_{lm}^{x-} R_{l-1,m-1} \tag{21a}$$

$$\partial_y R_{lm} = c_{lm}^{y+} R_{l-1,-(m+1)} + c_{lm}^{y-} R_{l-1,-(m-1)} \tag{21b}$$

$$\partial_z R_{lm} = c_{lm}^{z} R_{l-1,m} \tag{21c}$$

where

$$c_{lm} = \sqrt{\frac{(l+m-1)(l+m)}{4}\frac{2l+1}{2l-1}} \tag{22a}$$

$$c_{lm}^{x+} = \begin{cases} -c_{l,-m} & m \le -2 \\ 0 & m = -1 \\ \sqrt{2}\, c_{l,0} & m = 0 \\ c_{l,-m} & m \ge 1 \end{cases} \tag{22b}$$

$$c_{lm}^{x-} = \begin{cases} c_{lm} & m \le -1 \\ 0 & m = 0 \\ -\sqrt{2}\, c_{l,1} & m = 1 \\ -c_{lm} & m \ge 2 \end{cases} \tag{22c}$$

$$c_{lm}^{y+} = \begin{cases} -c_{l,-m} & m \le -2 \\ -\sqrt{2}\, c_{l,1} & m = -1 \\ \sqrt{2}\, c_{l,0} & m = 0 \\ c_{l,-m} & m \ge 1 \end{cases} \tag{22d}$$

$$c_{lm}^{y-} = \begin{cases} -c_{l,m} & m \le -1 \\ 0 & m = 0,\ 1 \\ c_{l,m} & m \ge 2 \end{cases} \tag{22e}$$

$$c_{lm}^{z} = \sqrt{(l^2 - m^2)\frac{2l+1}{2l-1}} \tag{22f}$$

to simplify the RO vertical recurrence relation (RO-VRR) eq 29 in Limpanuparb et al.[6] to

$$\begin{aligned}[(\mathbf{a}+\mathbf{1}_j)\mathbf{0}|nlm]^{(p)} &= (P_j - A_j)[\mathbf{a0}|nlm]^{(p)} + P_j[\mathbf{a0}|nlm]^{(p+1)} \\ &+ \frac{a_j}{2\zeta}\{[(\mathbf{a}-\mathbf{1}_j)\mathbf{0}|nlm]^{(p)} + [(\mathbf{a}-\mathbf{1}_j)\mathbf{0}|nlm]^{(p+1)}\} \\ &- \frac{\delta_{j,x}}{\lambda_n}\{c_{lm}^{x+}[\mathbf{a0}|n, l-1, m+1]^{(p+1)} \\ &- c_{lm}^{x-}[\mathbf{a0}|n, l-1, m-1]^{(p+1)}\} \\ &- \frac{\delta_{j,y}}{\lambda_n}\{c_{lm}^{y+}[\mathbf{a0}|n, l-1, -(m+1)]^{(p+1)} \\ &+ c_{lm}^{y-}[\mathbf{a0}|n, l-1, -(m-1)]^{(p+1)}\} \\ &- \frac{\delta_{j,z}}{\lambda_n}c_{lm}^{z}[\mathbf{a0}|n, l-1, m]^{(p+1)}\end{aligned} \tag{23}$$

If $P = 0$, the RO-VRR (eq 23) still holds, but we observe that $[\mathbf{00}|nlm]^{(p)} = 0$ for $l + p > a + b$. If $\lambda_n = 0$, the RO-VRR (eq 23) collapses to standard Boys recurrence relation (VRR)[27]

$$[(\mathbf{a}+\mathbf{1}_j)\mathbf{0}| = (P_j - A_j)[\mathbf{a0}| + \frac{a_j}{2\zeta}[(\mathbf{a}-\mathbf{1}_j)\mathbf{0}| \tag{24}$$

and only $p = l = m = 0$ is required.

Following the suggestion in the previous paper,[6] we use the equations described above to generate $[\mathbf{a0}|nlm]$, $[(\mathbf{a}+\mathbf{1})\mathbf{0}|nlm]$, ..., $[(\mathbf{a}+\mathbf{b})\mathbf{0}|nlm]$ integrals and contract them into $(\mathbf{a0}|nlm)$, $((\mathbf{a}+\mathbf{1})\mathbf{0}|nlm)$, ..., $((\mathbf{a}+\mathbf{b})\mathbf{0}|nlm)$. Then we apply standard horizontal recurrence relation (HRR)[28]

$$(\mathbf{a}(\mathbf{b}+\mathbf{1}_j)| = ((\mathbf{a}+\mathbf{1}_j)\mathbf{b}| + (A_j - B_j)(\mathbf{ab}| \tag{25}$$

This yields the desired $(\mathbf{ab}|nlm)$ class as a final result. The scheme described above is also readily applicable to the Bessel resolution of the Coulomb operator.[4] The only change is in the precomputed λ_n and q_n, which are much simpler for the Coulomb operator.

3. NUMERICAL RESULTS

Our test cases comprise typical biomolecules (water clusters,[29] polypeptides,[30] and triglyceride[31]), a conducting system (buckminsterfullerene[32]), and a weakly interacting system (helium cluster[33]). Geometries are described in the references given here. All calculations were run on a single core of a 2.93 GHz Intel Nehalem X5570 CPU with 24 GB DDR3-1333 memory. We compared the performance and accuracy of our code against Q-Chem 4.0.0.1.[34] We use MOs from diagonalization of the core Hamiltonian and Cartesian orbitals for all calculations in this section.

To assess accuracy, we report Frobenius norms $\|\mathbf{J} - \mathbf{J}^{REF}\|$, $\|\mathbf{K} - \mathbf{K}^{REF}\|$, maximum deviations $\max|J_{\mu\nu} - J_{\mu\nu}^{REF}|$, $\max|K_{\mu\nu} - K_{\mu\nu}^{REF}|$, and relative error in Coulomb and exchange energies

$$\varepsilon = -\log_{10}\left|\frac{E - E^{REF}}{E^{REF}}\right| \tag{26}$$

where "REF" refers to a calculation at THRESH = 14 and the energies are defined below.

dx.doi.org/10.1021/ct301110y | J. Chem. Theory Comput. XXXX, XXX, XXX–XXX

Table 1. Error in J and K Matrices and Energies Calculated by the Resolution and Q-Chem at Various ω and THRESH[a]

			RO				Q-Chem	
molecule/basis set	ω	THRESH	ΔJ	ΔK	ε_J	ε_K	ε_J	ε_K
triacetin/6-311G	0.1	6	11.91 (4.99)	12.50 (7.32)	9.54	7.98	7.1	5.8
triacetin/cc-pVDZ	0.1	6	10.71 (4.85)	13.20 (6.82)	9.26	7.99	6.0	6.1
triacetin/cc-pVTZ	0.1	6	10.53 (4.37)	14.18 (6.69)	8.38	7.86	6.5	5.4
$(H_2O)_{10}$/cc-pVDZ	0.1	6	9.30 (6.20)	11.31 (8.34)	8.58	7.80	6.29	6.13
	0.1	7	11.63 (7.20)	12.86 (8.76)	11.38	9.60	7.31	8.52
	0.1	8	12.71 (8.23)	14.15 (8.76)	>12.68	>10.45	8.82	8.07
	0.5	6	10.96 (5.95)	11.27 (7.29)	8.82	7.73	6.36	6.42
	0.5	7	13.17 (6.93)	12.91 (8.59)	10.47	9.32	7.38	7.48
	0.5	8	14.04 (7.96)	13.42 (8.77)	11.11	9.95	8.80	8.46
C_{60}/STO-3G	0.1	6	9.84 (5.17)	10.24 (7.32)	8.56	7.11	5.12	5.08
	0.1	7	12.46 (6.15)	11.54 (8.31)	11.28	8.43	5.98	7.57
	0.1	8	13.14 (9.20)	12.90 (9.62)	12.44	9.82	7.68	7.48
	0.5	6	9.63 (4.97)	13.01 (7.06)	8.54	8.21	5.11	5.03
	0.5	7	12.31 (5.96)	12.34 (8.07)	10.60	8.77	5.96	6.30
	0.5	8	14.06 (9.47)	14.16 (9.81)	11.99	10.38	7.67	8.35
He_9/aug-cc-pVQZ	0.1	6	11.34 (5.25)	12.40 (6.56)	7.68	6.64	7.73	7.45
	0.1	7	12.04 (6.55)	13.67 (6.56)	8.39	7.68	8.44	8.56
	0.1	8	13.37 (7.48)	15.28 (6.56)	9.56	8.80	9.84	8.85
	0.5	6	12.18 (5.04)	12.68 (6.67)	8.22	7.78	7.70	7.72
	0.5	7	13.20 (6.35)	13.84 (6.67)	9.59	9.21	8.52	9.40
	0.5	8	14.51 (7.28)	14.12 (6.67)	11.08	>10.36	9.82	8.98

[a]The Δ columns show $-\log_{10}\|\mathbf{J}-\mathbf{J}^{REF}\|$ ($-\log_{10}\max|J_{\mu\nu}-J^{REF}_{\mu\nu}|$) or their counterpart for **K**. Cases where energies agree to the 10th decimal place are indicated by >.

Table 2. J and K Matrices Generation Time of RO and Conventional Algorithms, THRESH = 6

								SCF time/seconds				
								RO				
molecule	basis set	ω	O	N	R	$\mathcal{N}'$	$\mathcal{L}$	aux	J	K	total	Q-Chem[a]
triacetin	6-31G*	0.1	58	295	25.26	6	7	0.58	0.07	0.88	1.53	2.44
″	″	0.2	″	″	″	9	14	2.13	0.31	4.67	7.11	″
″	″	0.5	″	″	″	18	34	19.82	3.11	47.98	70.91	″
″	″	1.0	″	″	″	33	67	144.54	20.77	318.86	484.17	″
$(H_2O)_5$	cc-pVDZ	0.3	25	125	16.19	9	13	0.54	0.07	0.48	1.09	0.53
″	cc-pVTZ	″	″	325	″	″	″	2.04	0.33	3.02	5.39	5.90
″	cc-pVQZ	″	″	700	″	″	″	7.76	1.34	13.75	22.85	99.50
$(H_2O)_{10}$	cc-pVDZ	″	50	250	18.97	9	16	2.22	0.31	3.45	5.98	2.91
″	cc-pVTZ	″	″	650	″	″	″	9.16	1.60	24.02	34.78	37.20
″	cc-pVQZ	″	″	1400	″	″	″	35.73	6.97	109.56	152.26	510.00
1D-alanine$_4$	6-311G	0.3	77	326	34.52	15	27	10.60	2.06	47.03	59.69	4.60
3D-alanine$_4$	″	″	″	″	22.91	11	19	5.40	0.92	16.89	23.21	6.25
1D-alanine$_8$	″	″	153	646	61.64	24	46	93.96	17.39	1400.22	1511.57	20.70
3D-alanine$_8$	″	″	″	″	30.56	13	24	24.84	4.61	226.71	256.16	37.10

[a]AOints time from full Coulomb operator is reported here. This is a good approximation for conventional long-range **J** and **K** calculation time as the number of integrals required is roughly the same.

$$E_J = \frac{1}{2}\sum_{\mu\nu}^{N^2} D_{\mu\nu}J_{\mu\nu} \tag{27}$$

$$E_K = -\frac{1}{8}\sum_{\mu\nu}^{N^2} D_{\mu\nu}K_{\mu\nu} \tag{28}$$

3.1. Accuracy Test. We first explore how RO THRESH performs and compare it with traditional two-electron integral THRESH in Q-Chem. Four representative examples given in Table 1 show that (a) the accuracy of RO approximation at a given THRESH remains more or less the same when different basis sets are used and (b) the accuracy of RO energies can be controlled by THRESH in a very similar manner to a conventional algorithm.

3.2. Timing Test. To compare the performance of RO and conventional algorithms, we timed one HF SCF cycle at THRESH = 6 and tabulated the results in Table 2. The RO calculation consists of three tasks: generation of auxiliaries and **J** and **K** matrix calculations. The majority of RO computation cost lies in two DGEMM calls from **K** matrix calculations and the generation of auxiliary integrals while the **J** matrix calculation time is relatively small (<6%).

dx.doi.org/10.1021/ct301110y | J. Chem. Theory Comput. XXXX, XXX, XXX−XXX

From the triacetin result, we observe that the RO parameters $\mathcal{N}'$ and $\mathcal{L}$ are sensitive to ω, and as a result, the computational time increases rapidly with ω. Therefore, we choose $\omega = 0.3$, an optimized value in Chai and Head-Gordon ωB97XD[15] for all other cases. A series of calculations on water clusters shows that RO is much faster than a conventional calculation when employed in high quality basis (cc-pVQZ) calculations. It is obvious from previous sections that the RO parameters $\mathcal{N}'$ and $\mathcal{L}$ do not depend upon basis set; as a result RO calculations scale only quadratically with the basis set size. This compares very favorably with the conventional methods, whose cost grows quartically with the basis set size for a fixed molecule.

We then look at the effect of molecular shape on the cost of RO calculation in polyalanine test cases. Unlike traditional algorithms where various cutoff strategies are very effective in 1D chain-like molecules, RO is more effective for 3D globular molecules. This is due to the fact that the molecular radius R is an important determining factor for $\mathcal{N}'$ and $\mathcal{L}$.

We note that these results are only preliminary and may be improved further by various approaches. One possibility is to use nonrectangular truncation of eq 2. There are three subscript variables n, l, and m that may be independently fine-tuned, and eq 3 is just the simplest form of truncation for general calculations. Rod-like 1D molecule calculations may benefit from additional m-truncation. The other possibility is to take advantage of the sparsity of the auxiliary integral matrix 6 in the computation of eqs 9−12. Therefore, the results presented here should be viewed as indicating trends rather than the best possible computation times. We expect reduced CPU times in a well-optimized implementation of RO.

4. CONCLUDING REMARKS

Our implementation of the resolution of the long-range Ewald operator has shown that the cost of HF **J** and **K** matrix calculation using high quality basis sets can be significantly reduced. Our algorithm scales only quadratically with respect to basis set size (for a fixed molecule) and works best for compact globular molecules, for which traditional cutoff strategies are ineffective. The performance of the RO algorithm can be improved further by exploiting the short-range nature of exchange interaction to reduce $\mathcal{N}'$ and by making use of parallel computation. These possibilities will be explored in our future papers.

AUTHOR INFORMATION

Corresponding Author

*E-mail: taweetham.lim@mahidol.ac.th.

Notes

The authors declare the following competing financial interest(s): P. M. W. Gill is part owner and president of Q-Chem Inc.

ACKNOWLEDGMENTS

Thanks to Dr. David Grove at IBM Watson Research Center and Dr. Andrew Gilbert at ANU Research School of Chemistry. This work was partially supported by the Australian Research Council and IBM through Linkage grant LP0989872, and by the NCI National Facility at the ANU.

REFERENCES

(1) Varganov, S. A.; Gilbert, A. T. B.; Deplazes, E.; Gill, P. M. W. *J. Chem. Phys.* **2008**, *128*, 201104.
(2) Gill, P. M. W.; Gilbert, A. T. B. *J. Chem. Phys.* **2009**, *356*, 86−90.
(3) Limpanuparb, T.; Gill, P. M. W. *J. Phys. Chem. Chem. Phys.* **2009**, *11*, 9176−9181.
(4) Limpanuparb, T.; Gilbert, A. T. B.; Gill, P. M. W. *J. Chem. Theory Comput.* **2011**, *7*, 830−833.
(5) Limpanuparb, T.; Gill, P. M. W. *J. Chem. Theory Comput.* **2011**, *7*, 2353−2357.
(6) Limpanuparb, T.; Hollett, J. W.; Gill, P. M. W. *J. Chem. Phys.* **2012**, *136*, 104102.
(7) Gill, P. M. W.; Adamson, R. D.; Pople, J. A. *Mol. Phys.* **1996**, *88*, 1005−1009.
(8) Yanai, T.; Tew, D. P.; Handy, N. C. *Chem. Phys. Lett.* **2004**, *393*, 51−57.
(9) Heyd, J.; Scuseria, G. E.; Ernzerhof, M. *J. Chem. Phys.* **2003**, *118*, 8207−8215.
(10) Izmaylov, A. F.; Scuseria, G. E.; Frisch, M. J. *J. Chem. Phys.* **2006**, *125*, 104103.
(11) Krukau, A. V.; Vydrov, O. A.; Izmaylov, A. F.; Scuseria, G. E. *J. Chem. Phys.* **2006**, *125*, 224106.
(12) Brothers, E. N.; Izmaylov, A. F.; Normand, J. O.; Barone, V.; Scuseria, G. E. *J. Chem. Phys.* **2008**, *129*, 011102.
(13) Sato, T.; Tsuneda, T.; Hirao, K. *J. Chem. Phys.* **2007**, *126*, 234114.
(14) Vydrov, O. A.; Heyd, J.; Krukau, A. V.; Scuseria, G. E. *J. Chem. Phys.* **2006**, *125*, 074106.
(15) Chai, J. D.; Head-Gordon, M. *Phys. Chem. Chem. Phys.* **2008**, *10*, 6615−6620.
(16) Appel, A. W. *SIAM J. Sci. Stat. Comput.* **1985**, *6*, 85−103.
(17) Rokhlin, V. *J. Comput. Phys.* **1985**, *60*, 187−207.
(18) Greengard, L. *The Rapid Evaluation of Potential Fields in Particle Systems*; MIT Press: Cambridge, MA, 1987.
(19) White, C. A.; Johnson, B. G.; Gill, P. M. W.; Head-Gordon, M. *Chem. Phys. Lett.* **1996**, *253*, 268−278.
(20) Adamson, R. D.; Dombroski, J. P.; Gill, P. M. W. *J. Comput. Chem.* **1999**, *20*, 921−927.
(21) Limpanuparb, T. Applications of Resolutions of the Coulomb Operator in Quantum Chemistry. Ph.D. dissertation, Australian National University, Acton, Australian Capital Territory, Australia, 2012. http://hdl.handle.net/1885/8879 (accessed Jan. 2013).
(22) Dominici, D. E.; Gill, P. M. W.; Limpanuparb, T. *Proc. R. Soc. London, Ser. A* **2012**, *468*, 2667−2681.
(23) Saraswat, V.; Bloom, B.; Peshansky, I.; Tardieu, O.; Grove, D. *X10 Language Specification*, version 2.3; IBM: Armonk, NY, 2012.
(24) Dongarra, J. J.; du Croz, J.; Hammarling, S.; Duff, I. *ACM T. Math. Software* **1990**, *16*, 1−17.
(25) ANUChem. http://cs.anu.edu.au/~Josh.Milthorpe/anuchem.html (accessed Jan. 8, 2013).
(26) Milthorpe, J.; Ganesh, V.; Rendell, A.; Grove, D. *Proceedings of the 25th IEEE International Parallel & Distributed Processing Symposium (IPDPS)*; IEEE: 2011; pp 1080−1088
(27) Boys, S. F. *Proc. R. Soc. London* **1950**, *A200*, 542−554.
(28) Head-Gordon, M.; Pople, J. A. *J. Chem. Phys.* **1988**, *89*, 5777−5789.
(29) The Cambridge Cluster Database, *ab initio* Optimized $(H_2O)_N$ Clusters. http://www-wales.ch.cam.ac.uk/wales/CCD/anant-watcl.html (accessed Jan. 8, 2013).
(30) DiStasio, R. A.; Jung, Y.; Head-Gordon, M. *J. Chem. Theory Comput.* **2005**, *1*, 862−876.
(31) Limpanuparb, T.; Punyain, K.; Tantirungrotechai, Y. *J. Mol. Struct.: THEOCHEM* **2010**, *955*, 23−32.
(32) Ufimtsev, I. S.; Martinez, T. J. *J. Chem. Theory Comput.* **2009**, *5*, 1619−2628.
(33) Boman, L.; Koch, H.; Sánchez de Merás, A. *J. Chem. Phys.* **2008**, *129*, 134107.
(34) Krylov, A.; Gill, P. *WIREs Comput. Mol. Sci.* 2013; DOI: 10.1002/wcms.1122.